

Thermal Phase Transitions of Substituted Poly[bis(4-R-phenoxy)phosphazenes]

M. A. Gomez,* C. Marco, and J. G. Fatou

*Instituto de Ciencia y Tecnologia de Polimeros, Juan de la Cierva 3,
28006 Madrid, Spain*

T. N. Bowmer

Bell Communications Research, Inc., Red Bank, New Jersey 07701

R. C. Haddon and S. V. Chichester-Hicks

AT&T Bell Laboratories, Murray Hill, New Jersey 07974

Received June 12, 1990; Revised Manuscript Received October 24, 1990

ABSTRACT: The phase transitions observed in two substituted poly[bis(4-R-phenoxy)phosphazenes] ($R = \text{OCH}_3$ (PBMOPP) and SCH_3 (PBMTTP)) have been studied by DSC, X-ray diffraction, and optical microscopy. Both polymers exhibit thermotropic behavior. The influence of the size and polarity of the substituents on the thermal transitions and on the mesophase formation has been analyzed and compared with that of other substituted polyphosphazenes. The kinetics of crystallization from the mesophase and from the isotropic melt have also been analyzed for PBMOPP, PBMTTP, and poly[bis(4-ethylphenoxy)phosphazene] (PBEPP). The kinetic studies have shown that the isotherms have a behavior similar to that found in the crystallization of homopolymers, with an Avrami exponent of $n = 3$ for PBMOPP and PBMTTP. This exponent can be interpreted as a nucleation-controlled process with a two-dimensional growth. A strong dependence of the crystallization kinetics on the conditions of the mesophase formation has been observed, particularly the temperature of the mesophase before crystallization. In PBEPP, changes in crystallization rates and in final crystallinity for the same crystallization temperatures have been obtained depending on whether the polymer is crystallized from the mesomorphic or the isotropic state. Finally, with the assumption that the growth of the mesophase is similar to polymer crystallization, the temperature coefficient of the transformation process has been determined. Values of this coefficient are found to be related to the bulkiness and polarity of the substituents in our polyphosphazenes.

Introduction

Polyphosphazenes (PPPZ's) are a broad class of inorganic polymers with a backbone consisting of alternating P and N atoms. Due to the synthetic versatility of the precursor [poly(dichlorophosphazene), $(\text{NPCl}_2)_x$],¹⁻⁴ a wide variety of different organic or organometallic side groups can be attached to the polymer chain. This results in several important properties,²⁻¹⁴ such as excellent mechanical and chemical stability properties, unusual thermal properties, and biocompatibility, some of which may have commercial relevance. The high level of interest in these polymeric systems is reflected in a large number of recent publications.¹⁵⁻²²

Most semicrystalline polyphosphazenes are known to have three transitions:²³ the glass transition, T_g , the thermotropic transition from crystal to mesophase, called $T(1)$, and the mesophase to isotropic melt transition, T_m . This thermotropic behavior is one of the most interesting properties of polyphosphazenes. It has also been found^{18,19,24-26} that some PPPZ's whose substituents have the structures $\text{OC}_6\text{H}_4\text{R}$ have multiple crystalline forms below $T(1)$, the crystal-liquid crystal transition, depending on crystallization conditions. A number of morphological and structural studies of semicrystalline polyphosphazenes have been made in order to examine and understand the nature of the transformation that takes place during the thermotropic transition,¹⁵⁻¹⁹ especially in the case of poly-(diphenoxyphosphazene).

In previous work,^{27,28} we have reported a motional and structural study of the phase transitions observed in poly-[bis(4-ethylphenoxy)phosphazene] (PBEPP) and the glass transition of poly[bis(4-*tert*-butylphenoxy)phosphazene] (PBTBPP) by solid-state NMR, DSC, and X-ray tech-

niques. The side-chain groups play a very important role in determining the physical properties of these polymers, because of the inherent backbone flexibility. Thus, thermal and mechanical behavior depends on the nature of the substituents on the P atoms.

In this work, we report on the phase transitions associated with the poly[bis(4-R-phenoxy)phosphazenes] shown in Figure 1. An extensive characterization of these phase transitions has been carried out by DSC, X-ray diffraction, optical microscopy, and thermooptical analysis. Comparison of the results observed for these polymers with those obtained for PBEPP permits the study of the influence of the size and polarity of the substituent on the thermal transitions as well as its effect on the mesophase formation.

Information about the kinetics of mesophase formation in polymers is very scarce, although such studies may help to provide an understanding of the nature of the mesomorphic states. In the case of polyphosphazenes, several kinetic studies have been pioneered by Magill and co-workers using different techniques.^{13,22,29,30} In the present work, the kinetics of crystallization from the mesophase and from the isotropic melt have also been analyzed and compared for different polyphosphazenes.

Experimental Section

Synthesis and Characterization. All the polymers were prepared by a substitution reaction of the appropriate thallium aryl oxide salts on poly(dichlorophosphazene). Full details of the preparation have been given elsewhere.³¹

Elemental analysis of the polymers showed <0.2% residual chlorine. The ³¹P NMR spectra were in agreement with this high level of chlorine replacement. The IR spectra exhibited the

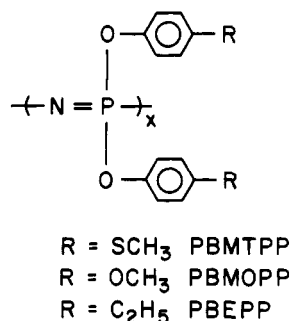


Figure 1. Chemical structure of PBMOPP, PBMTTP, and PBEPP.

characteristic polyphosphazene P-N stretching vibration at about 1200 cm⁻¹. The ring breathing mode at about 1500 cm⁻¹ was also evident. Gel permeation chromatography indicated a number-average molecular weight of the order of 10⁶ for all polymers.

Physical Properties. Perkin-Elmer DSC 4 and Mettler TA 3000-DSC 30 differential scanning calorimeters were used to measure the thermal properties of the polyphosphazene samples. Although the heating rate was always 10 °C/min, various cooling rates were selected to study the transitions. The first DSC runs were obtained from samples precipitated from solution, but subsequent runs were carried out with samples heated between $T(1)$ and T_m . In a few cases samples were heated to T_m .

In some cases, crystallization kinetics studies were carried out either from the isotropic state or from the mesophase. The samples were cooled at 32 °C/min until the desired crystallization temperature was reached and the corresponding crystallization exotherms scanned as a function of time. The partial areas corresponding to a given transformation percentage were determined on a PE 7700 computer with Perkin-Elmer DSC-7 kinetic software.

Microscopy studies were carried out with a Reichert transmitted-light binocular microscope fitted with a photomonitor to a Mettler FP80 central processor; the analog output was recorded on a strip-chart recorder for thermo-optical analysis (TOA). The melting and clearing temperatures were observed for different cooling and heating rates with a Mettler FP82 hot stage. Films for microscopy and TOA were prepared by heating the polymers above $T(1)$ and cooling to room temperature.

Wide-angle X-ray (WAXS) investigations of films of the polymers were carried out at different temperatures, using a Philips Geiger counter X-ray diffractometer. The diagrams were recorded in the 2θ range between 5 and 40° with Ni-filtered Cu $K\alpha$ radiation at $2^\circ/\text{min}$ rates. Films were also prepared by molding the polymers at temperatures above the $T(1)$ temperature and then crystallizing under specified conditions.

Results and Discussion

Poly[(aryloxy)phosphazenes] are semicrystalline polymers, and their crystallinity and thermal transitions depend on the chemical structure, on the conditions of the sample preparation, and on the thermal history. In various poly[(aryloxy)phosphazenes], the isotropization temperature can approach or exceed the initial temperature for thermal degradation, which will prevent analysis of the transition to the isotropic state and crystallization studies from the completely amorphous state. The individual properties of the two new polyphosphazenes will be examined first and then compared with the results from other previously studied polyphosphazenes. The kinetics of crystallization from the mesophase and from the isotropic melt will also be analyzed.

(a) Poly[bis(4-methoxyphenoxy)phosphazene] (PBMOPP). Figure 2 shows the DSC scans of PBMOPP for different heating-cooling processes. The sample precipitated from solution (run 1) showed a glass transition at 16 °C and two endotherms located at 115 and 141 °C, respectively. The existence of these two transitions may

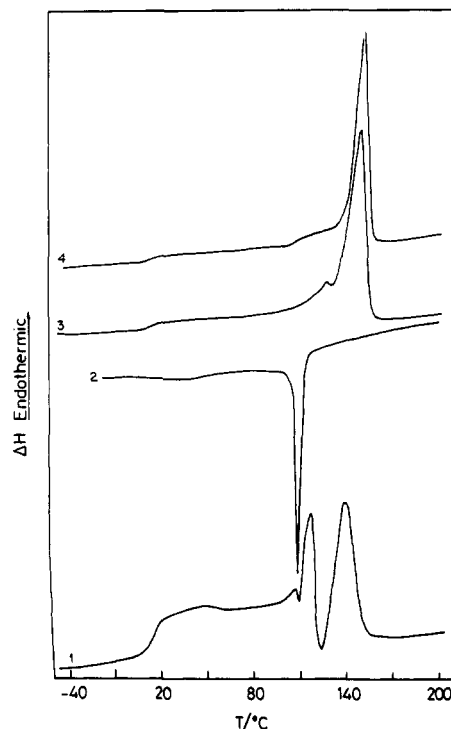


Figure 2. DSC curves for PBMOPP with different thermal treatments (indicated in Table I).

Table I
Thermal Transition Data of PBMOPP from DSC and TOA

run	remarks	T_g , °C	$\frac{\Delta C_p(T_g)}{\text{cal}\cdot\text{g}^{-1}\cdot\text{°C}^{-1}}$	$T(1)$, °C	$\frac{\Delta H(T(1))}{\text{cal}\cdot\text{g}^{-1}}$	T_m^a , °C	$1-\lambda^b$
1	original	16	0.044	115-141	3.5	340	68
2	crystallization	20		114	9.5		
3	melting	16	0.025	151	11.2		82
4	isotherm (100 °C)	15	0.011	152	12.4		91
5	quenching	15	0.016	151	12.1		88

^a From TOA. ^b Calculated as indicated in the text.

be assigned to either (1) the existence of two crystalline forms or (2) the presence of different crystallite sizes which cause the process of melting and further recrystallization and melting. The DSC measurements by themselves do not allow us to discriminate between these two possibilities.

Upon cooling from 200 °C at 10 °C/min (run 2), a crystallization exotherm with a peak at 114 °C was observed, followed by a steplike change at 20 °C, corresponding to the glass transition. If the sample was subsequently heated at 10 °C/min (run 3) to 200 °C, the glass transition was observed, followed by a melting peak at 151 °C with a minor shoulder at 125 °C. The heat of fusion associated with the 151 °C transition was small relative to other semicrystalline polymers, 46.8 J·g⁻¹ (11.2 cal·g⁻¹). However, it was about 8.4 J·g⁻¹ (2 cal·g⁻¹) more than the heat obtained in run 2 (see Table I). This is probably an indication of the crystallization in run 2 of low molecular weight species which subsequently causes the shoulder at 125 °C during the melting process.

The thermal behavior of PBMOPP did not depend strongly on prior thermal history with the exception of the first run. When the sample was isothermally crystallized from 200 °C at 100 °C for 48 h and then cooled to -50 °C at a cooling rate of 10 °C/min, the heating run (4) showed the same glass transition and the peak at 152 °C with a shoulder at 125 °C as was observed after the cooling process in run 2.

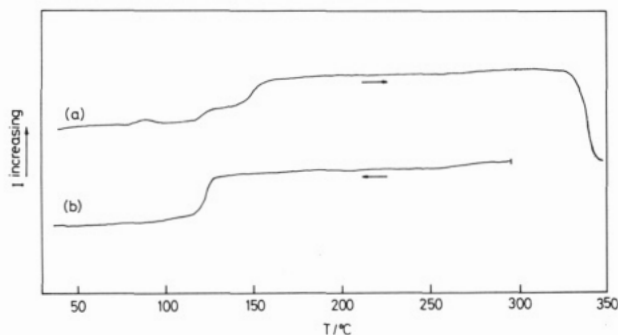


Figure 3. Thermo-optical analysis of PBMOPP: (a) heating; (b) cooling.

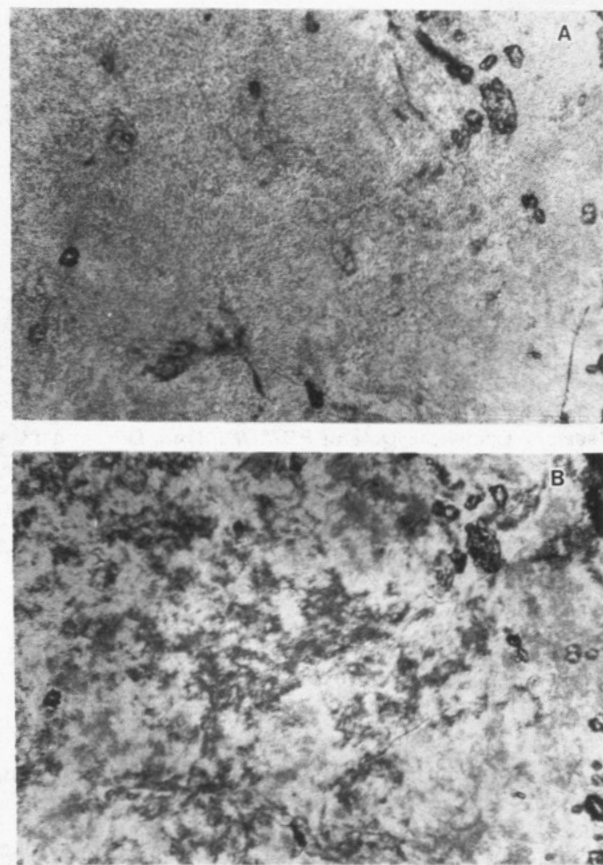


Figure 4. Optical microscopy photographs of PBMOPP taken at (A) 25° and (B) 162 °C (heating).

The transition at the higher temperature corresponded to the crystal-liquid crystal transition, $T(1)$, as will be demonstrated by optical microscopy and X-ray results. No other transitions were observed upon heating to 350 °C, the temperature at which degradation of the sample starts.³²

The transitions were also observed by thermo-optical analysis between room temperature and 350 °C at a heating rate of 10 °C/min for a sample cooled from 180 °C to room temperature. Two intensity gains were found at 125 and 155 °C, and an intensity loss starting at 340 °C, corresponding to the clearing temperature (Figure 3a), was observed. At higher temperatures the sample degraded. When a new sample prepared in the same manner was cooled from 300 °C at 10 °C/min, a loss in light intensity was found at 130 °C, corresponding to the crystallization of this polymer (Figure 3b).

In Figure 4, microphotographs, obtained during the scan depicted in Figure 3a, are shown. At room temperature there was only a slight birefringence, which increased at

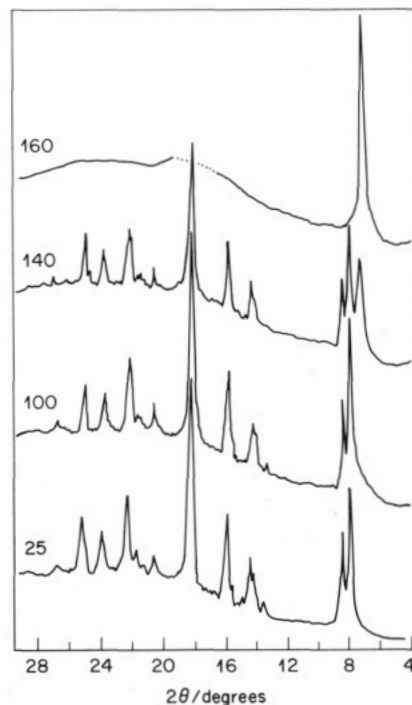


Figure 5. X-ray diffractograms of PBMOPP at different temperatures.

140 °C and was clearly observed at 160 °C, typical of a transformation from the crystalline to the liquid crystalline state.

In Figure 5, wide-angle X-ray diffraction patterns of PBMOPP at different temperatures are shown for a sample cooled from 180 °C, above $T(1)$, to room temperature. This sample presented reflections at $2\theta = 8.0, 8.6, 14.4, 15.9, 18.3, 20.6, 22.2, 23.9,$ and 25.2° associated with inter- and intramolecular order in the three-dimensional crystalline structure. The reflections remained at temperatures up to 120 °C, indicating that there was a single-crystalline form. Some thermotropic polyphosphazenes exhibit polymorphism. It has been shown¹⁹ that in some cases a monoclinic form transforms into an orthorhombic form through the thermotropic state. However, this was not the situation for PBMOPP, at least with this thermal treatment, and therefore the shoulder in the melting endotherm must originate from the fusion of smaller crystallites, formed from low molecular weight species in the sample. However, additional structural studies in PBMOPP will be the subject of further work.

At 140 °C, the X-ray pattern showed a decrease in the intensity of the crystalline reflections, with the appearance of a reflection at $2\theta = 7.4^\circ$, assigned to the mesophase. At temperatures above $T(1)$, i.e., 180 °C, only this reflection was observed, which persisted up to 300 °C. The reflection at low angles indicated the existence of intermolecular order, and the amorphous halo implied the absence of intramolecular order. These X-ray results coupled with the DSC and TOA results confirmed the existence of a mesophase.

As has been pointed out for some other polyphosphazenes,^{19,20} the structural transformation in PBMOPP takes place from a three-dimensionally ordered state to a two-dimensional pseudohexagonal form that involves unit cell expansion. The thermotropic state has considerable backbone motion and disorder of the backbone and side groups, as indicated by solid-state NMR studies.^{27,28,33}

The transition from liquid crystal to the isotropic liquid occurs at temperatures higher than 300 °C, with degra-

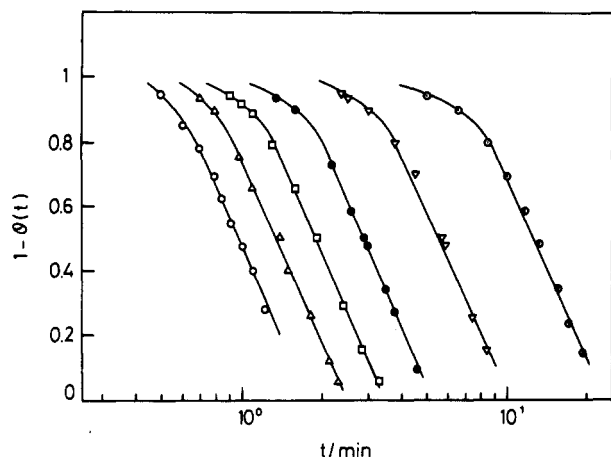


Figure 6. Extent of transformation versus log (time) curves for PBMOPP from the DSC isothermals at $T_c = 131$ (○), 132 (△), 133 (□), 134 (●), 135 (▽), and 136 °C (○).

dation starting almost at the same time that the clearing process takes place. This is one case in which T_m is very close to the decomposition temperature, as has been found in other polyphosphazenes.

The isothermal crystallization of PBMOPP was analyzed by calorimetry. The kinetics for three crystallization procedures may be considered for liquid crystals: (1) crystallization from the isotropic state to the mesomorphic range ($T(1) < T_c < T_m$), (2) crystallization of the sample from the isotropic state to a crystallization temperature below $T(1)$, and (3) crystallization from the mesomorphic state to a temperature below $T(1)$. However, the isotropic temperature is very close to the degradation temperature in PBMOPP, and no kinetic data from the isotropic state could be obtained. Therefore only isothermal crystallization experiments from the mesomorphic state were conducted. The initial temperature was 170 °C ($T(1) = 152$ °C) and the samples were cooled at 32 °C/min to a given crystallization temperature. Reproducible isotherms were obtained in the range 131–136 °C following the usual crystallization patterns described in the Experimental Section. The extent of transformation with log (time) curves for PBMOPP obtained from the DSC isotherms is shown in Figure 6.

A linear relation was obtained for the initial portion of the transformation in a plot of the crystallinity ($1 - \lambda$) vs time (Figure 7a). After deviations from linearity develop, the degree of crystallinity at very long times was independent of the crystallization temperature. This behavior has been obtained previously for the bulk crystallization of homopolymers.³⁴

Note that the maximum crystallinity reached was significantly lower than the crystallinity obtained when the sample was cooled from the mesomorphic state to room temperature. The significance of this crystallinity difference will be discussed later.

(b) Poly[bis(4-(methylthio)phenoxy)phosphazene] (PBMTTP). Figure 8 shows the DSC scan of a PBMTTP sample precipitated from solution (run 1) and heated to 200 °C. The steplike change at 40 °C was the glass transition, and an endothermic peak at 135 °C corresponded to the crystal–liquid crystal transition as will be demonstrated by X-ray and microscopy studies. The heat of fusion was rather small, 10.9 J·g⁻¹ (2.6 cal·g⁻¹). The glass transition observed in this scan indicated the existence of an orientational order, characteristic of a glassy liquid crystal at temperatures below T_g coexisting with a fraction of crystallized polymer. The existence of this latter phase was confirmed by the appearance of a $T(1)$

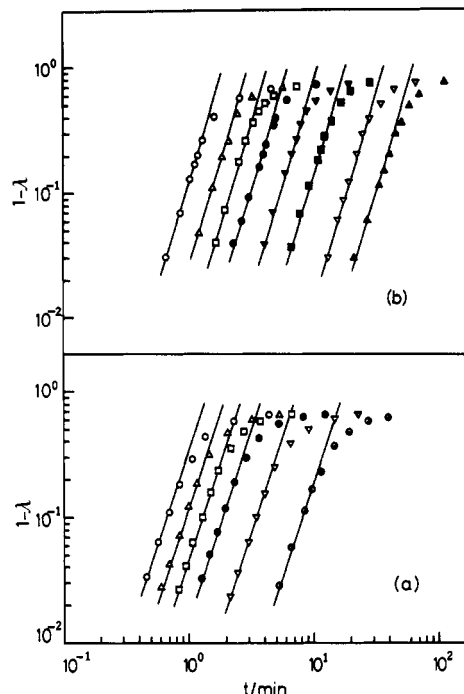


Figure 7. Plot of crystallinity ($1 - \lambda$) vs time: (a) PBMOPP at $T_c = 131$ (○), 132 (△), 133 (□), 134 (●), 135 (▽), and 136 °C (○); (b) PBMTTP at $T_c = 126$ (○), 127 (△), 127.5 (□), 128 (●), 128.5 (▽), 129 (■), 129.5 (▽), and 130 °C (△).

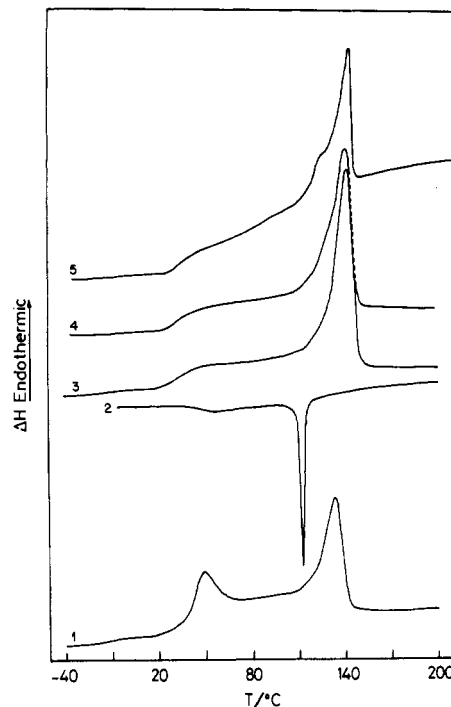


Figure 8. DSC curves for PBMTTP with different thermal treatments (indicated in Table II).

= 135 °C transition, and the existence of the mesophase below T_g will be demonstrated by X-ray analysis.

When the sample was crystallized during cooling from 200 to -50 °C at 10 °C/min (Figure 8, run 2), a crystallization peak was observed at 106 °C with a heat of transition of 20.5 J·g⁻¹ (4.9 cal·g⁻¹), and the glass transition was observed at 37 °C. During the subsequent heating cycle of this sample (run 3) to 200 °C, the glass transition was again observed at the same temperature, and the crystal–liquid crystal transition peak occurred at 142 °C. Similar results were obtained (run 4) if the sample

Table II
Thermal Transition Data of PBMTTP from DSC and TOA

run	remarks	T_c °C	$\Delta C_p(T_g)$, cal·g ⁻¹ ·°C ⁻¹	$T(1)$, °C	$\Delta H(T(1))$, cal·g ⁻¹	T_{m1} ^a , °C	$1-\lambda$ ^b
1	original	40	0.057	135	2.6	210	34
2	crystallization	37		106	4.9		
3	melting	37	0.028	142	5.1		67
4	after quenching	37	0.029	140	4.7		66
5	isotherm	36	0.035	110–139	4.7		58

^a From TOA. ^b Calculated as indicated in the text.

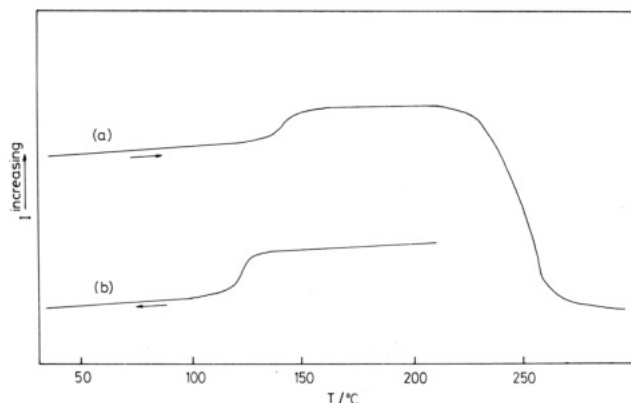


Figure 9. Thermooptical analysis of PBMTTP: (a) heating; (b) cooling.

was quenched from 200 to -50 °C (Table II).

However, if the sample was heated to 200 °C and isothermally crystallized at $T_c = 95$ °C for 24 h, the endotherm with a maximum at 139 °C showed a shoulder at 110 °C (run 5). This shoulder may be caused by the melting of smaller crystallites produced during the cooling run. Crystallization occurs in the range between 95 and 25 °C.

In all the described scans except run 5, the highest temperature in the heating cycles was 200 °C, without detecting the isotropic state. In run 5, the temperature was increased to 320 °C with degradation observed, starting at 240 °C. This observation agreed with thermal stability data previously determined for this polymer.³²

The TOA of a PBMTTP sample (Figure 9a) heated at 180 °C, above $T(1)$, and cooled to room temperature showed a gain in light intensity during heating at 150 °C, corresponding to $T(1)$, and an intensity loss, starting at 210 °C, corresponding to the clearing temperature. At higher temperatures, the sample degraded.

When a new sample of PBMTTP prepared under the same conditions was cooled from 200 °C at a cooling rate of 10 °C/min, the loss of intensity at 128 °C corresponded to the liquid crystal-crystal transition (Figure 9b).

Figure 10 shows the micrographs obtained for a sample cooled from 200 °C to room temperature. Thus micrograph 9A, obtained at 30 °C, i.e., below the glass temperature, presents a birefringence that is characteristic of the mesophase in the glassy state. The birefringence increases at temperatures above $T(1)$, as shown in micrograph 9B, obtained at 160 °C. A preliminary small-angle light scattering study of PBMOPP and PBMTTP has shown circular scattering patterns at room temperature which exclude a spherulitic morphology and suggest randomly oriented lamellae or rods.

Wide-angle X-ray patterns recorded as a function of temperature are shown in Figure 11 for a sample crystallized by cooling at 10 °C/min from 180 to 25 °C. At 25 °C, the pattern showed the existence of a poorly

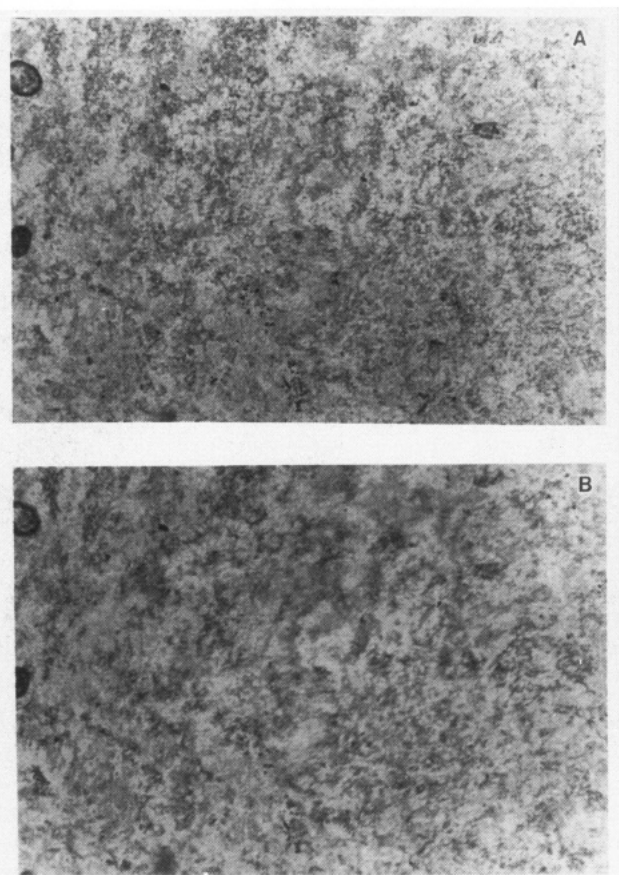


Figure 10. Optical microscopy photographs of PBMTTP at (A) 25 and (B) 160 °C.

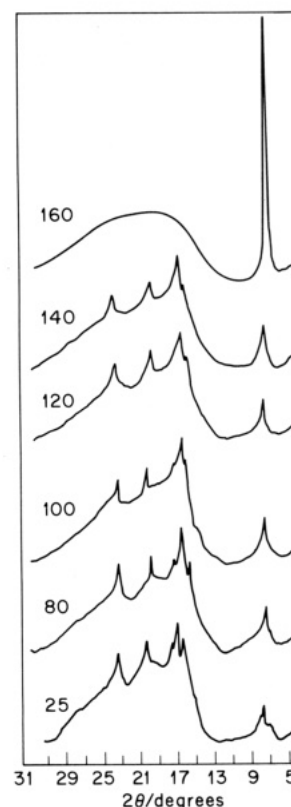


Figure 11. X-ray diffractograms of PBMTTP at different temperatures.

developed crystalline structure with reflections at $2\theta = 7.5, 16, 16.5, 20.2$, and 23.4 °. These reflections were associated with the crystalline order. Only the reflection at $2\theta = 7$ ° corresponded to the intermolecular order related

Table III
Thermal Transition Data of PBEPP from DSC and TOA

run	remarks	T_g , °C	$\Delta C_p(T_g)$, cal·g ⁻¹ ·°C ⁻¹	$T(1)$, °C	$\Delta H(T(1))$, cal·g ⁻¹	T_m , ^a °C	$1 - \lambda^b$
1	original	-16	0.039	90	3.12	240	68
2	crystallization	-16		60	2.0		
3	melting	-17.6	0.044	90	3.0		65
4	isotherm	-17.4	0.045	90.4	3.04		66
5	isotherm	-17	0.0475	90	3.0		65

^a From TOA. ^b Calculated as indicated in the text.

to a mesophase. There were no changes in the reflections between 30 and 140 °C.

Only at temperatures above the crystal-liquid crystal transition, i.e., 160 °C, did the intensity of the reflection at $2\theta = 7^\circ$, corresponding to the mesophase, increase and the reflections corresponding to the crystalline order disappear.

As noted for PBMOPP, the thermotropic transformation in PBMTTP implied a structural change from a crystalline state to a pseudohexagonal packing of cylinders occupied by mobile polymer chains.

The isothermal crystallization of PBMTTP was carried out from the mesomorphic phase as in the case of PBMOPP. It was not possible to conduct the crystallization from the isotropic state because in this polymer the degradation temperature and the melting temperature were also very close.

Therefore the crystallization studies were carried out from $T = 170^\circ\text{C}$ ($T(1) = 142^\circ\text{C}$) to a crystallization temperature range of 126–130 °C. As in the PBMOPP case, the isotherms were reproducible and a linear relation was found in the initial part of a plot of $1 - \lambda$ vs time (Figure 7b). After deviations from linearity develop, the results can be extrapolated to form a common straight line of small slope. The degree of crystallinity at long times was close to the crystallinity found when the sample was crystallized in a dynamic experiment from the mesomorphic state to room temperature, as will be discussed later.

(c) **Thermal Transitions.** The transition temperatures of PBMOPP and PBMTTP derived from the heating curves are summarized in Tables I and II and compared with those obtained for poly[bis(4-ethylphenoxy)phosphazene] (PBEPP) (Table III). First, the glass transition temperatures are virtually unaltered upon heating-cooling cycles at temperatures below T_m . PBMOPP has a lower glass transition than PBMTTP, but both present a higher T_g than PBEPP. The specific heat change at T_g , $\Delta C_p(T_g)$, for the starting material of PBMOPP and PBMTTP decreased upon several heating and cooling cycles through $T(1)$. These values are also indicated in Tables I and II. The lowest values correspond to the isothermally crystallized sample, in which the crystallinity was enhanced. Similar results have been discussed in several polyphosphazenes²³ and have been related to structural crystalline order associated with the chain-extended morphology.

The $T(1)$ transition is shifted toward higher temperatures when it is compared with the value obtained from the original sample. Also, the enthalpy associated with this transition increases.

Table IV lists values of T_g , d_{100} , and $T(1)$ for several polyphosphazenes with different lateral groups (R). It has been established that T_g is related linearly with the size of the lateral group.²⁰ Our results generally confirm this relation between T_g and the increasing bulkiness of the group on progressing from PBEPP to PBMTTP. However, T_g can also be affected by the polarity of the side group as shown by comparing the methoxy (PB-

Table IV
Structural and Thermal Data for Several Polyphosphazenes

poly[bis(R-phenoxy)- phosphazene]	R	T_g , °C	d_{100} , ^a Å	$T(1)$, °C
PBPP ^b	H	-4	11.4	159
PBMPP ^b	CH ₃	1		154
PBEPP	C ₂ H ₅	-16	12.8	90–110
PBMOPP	OCH ₃	15–20	12.1	152
PBMTTP	SCH ₃	40	12.6	142
PBPPP ^b	C ₆ H ₅	52	15.7	206

^a Interplanar distance in the thermotropic state. ^b From ref 20.

MOPP) and ethyl (PBEPP) polymers. The CH₃O substituent is approximately the same size as the ethyl substituent but the methoxy group is polar and therefore has the potential to increase interchain interactions. The increased dipole-dipole interactions may account for the increase in T_g from -16 °C (ethyl case) to +16 °C (methoxy case). However, if these values are compared with those for other polyphosphazenes, the T_g for PBEPP is significantly lower than the ones reported for PBPP and PBMPP. Extending the PPPZ series to other substituents may clarify the contributing factors to the glass transition.

The interplanar spacings in the thermotropic state of several polyphosphazenes are also indicated in Table IV. When the size of the side groups of each polyphosphazene is estimated based upon the atomic radius of each atom of the side groups, the interplanar distances in the thermotropic state of each polymer showed a linear dependence upon side-group dimension, as was described by Kojima and Magill.²⁰ This relation shows an increasing interplanar spacing with the group size in PBMOPP and PBT-MPP, with again the exception of PBEPP.

On the other hand, the quantities $\Delta C_p(T_g)$ and $\Delta H(T(1))$ can be related to the crystallinity as has been proposed.²³ Thus

$$\Delta C_p(T_g) = K_1(1 - \Delta H(T(1))/K_2) \quad (1)$$

where K_1 and K_2 are proportionality constants and can be calculated from a plot of $\Delta C_p(T_g)$ against $\Delta H(T(1))$.

The degree of crystallinity, $1 - \lambda$, is given by

$$1 - \lambda = \Delta H(T(1))/K_2 \quad (2)$$

or

$$\lambda = \Delta C_p(T_g)/K_1 \quad (3)$$

The crystallinities for PBMOPP and PBMTTP calculated from eqs 1 and 2 are included in Tables I and II.

Note that the crystallinity of the starting material differs substantially in these two polymers. PBMOPP presented a high crystallinity (68%), the highest that has been reported for polyphosphazenes under these conditions. However, original PBMTTP had a very low crystallinity (34%).

After cycling of the samples, the crystallinity increased in both cases (85% for PBMOPP and 65% for PBMTTP), although the values for PBMOPP were still higher than those for PBMTTP. The rather low crystallinity of the polyphosphazenes and, in particular, of PBMTTP has been attributed to the reduction of backbone flexibility due to the substituents. The effect of the side-group bulkiness plays an important role in determining this parameter.

In eq 1, Sun and Magill²³ pointed out that K_1 is a function of $T(1)$. Therefore, this equation does not imply that $\Delta C_p(T_g)$ and $\Delta H(T(1))$ are always proportional for all degrees of crystallinity. However, in spite of this limitation and in order to calculate relative crystallinities from the

plot of eq 1, $\Delta H(T(1))$ for the 100% crystalline polymer can be extrapolated. For PBMOPP this value is $\Delta H(T(1)) = 57.8 \text{ J}\cdot\text{g}^{-1}$ and for PBMTTP it is $31.8 \text{ J}\cdot\text{g}^{-1}$.

For comparative purposes, we have also considered poly[bis(ethylphenoxy)phosphazene] (PBEPP), and $\Delta C_p(T_g)$ and $\Delta H(T(1))$ have been measured under several conditions. Hence, the value of $\Delta H(T(1))_{100}$ was obtained. This corresponded to $19.2 \text{ J}\cdot\text{g}^{-1}$ and was lower than in the two previously mentioned cases. The crystallinity obtained for PBEPP was 68%.

Another interesting point is related to the transition temperatures. An empirical relationship has been proposed²⁰ for T_g , $T(1)$, and T_m for polyphosphazenes. It has been suggested that the form $(T_m - T_g)/(T_m - T(1))$ is proportional to $T(1)/T_m$ in the range $0.5 \leq T(1)/T_m \leq 0.9$. The polyphosphazenes studied in this work were consistent with this relationship.

Values of $\Delta H(T_m)$ cannot be determined from the calorimetric curves for PBMOPP and PBMTTP. It is known from other studies that $\Delta H(T_m)$ is in general very low, and it is very difficult to measure this parameter by DSC. It is approximately constant and independent of the thermal history. However, in the case of PBEPP, although it was observed by DSC, its precise quantitative determination was not possible.

(d) Crystallization Kinetics. The isothermal crystallization from either the molten state or the mesomorphic state has been considered. In general, polyphosphazenes have only been studied over a relatively narrow temperature range. It has been previously pointed out³⁵ that isothermal crystallization from the mesophase into the crystalline state occurs within a small range of temperatures below $T(1)$. A similar effect has been found in the formation of the mesophase from the isotropic state; the transformation occurs very rapidly, not too far below T_m . Thus, both processes take place in the vicinity of T_m and $T(1)$, and the transformation from the isotropic melt to the three-dimensional form seems to pass through the mesophase.

However, for PBMOPP and PBMTTP, the onset of the mesophase formation was not studied, because, as mentioned before, they undergo degradation when they are heated close to their melting temperatures. In those cases in which this transition occurs below the degradation temperature, the onset of the mesophase occurs several degrees below T_m . However, the enthalpy changes are very small. This is the situation for PBEPP, whose isothermal ordering from the melt is not detected in the region between $T(1)$ and T_m .

If the isothermal crystallization from the mesophase region to a crystallization temperature $T_c < T(1)$ was considered, it was possible to obtain quantitative data from calorimetric measurements. The rate at which crystallinity developed followed the universal pattern, which has been found in the bulk crystallization of polymers.³⁴

The rate of crystallization was strongly dependent on the crystallization temperature, but the shape of the isotherms and their superimposability indicated that this transformation was similar to crystallization from the melt and involved the concurrence of nucleation and growth processes. The mechanism was therefore independent of the transformation temperature.

The development of crystallinity in polymers has been described by the Avrami³⁶ and the free-growth approximations,³⁷ and these treatments were used in the analysis of our data. In spite of the simplifications introduced in these equations, they provide a convenient means to

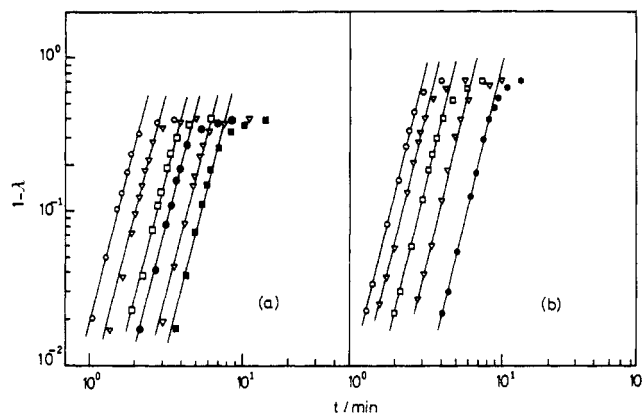


Figure 12. Plot of crystallinity ($1 - \lambda$) vs time for PBEPP: (a) crystallized from the mesophase at $T_c = 67$ (○), 69 (▽), 71 (□), 72 (●), 73 (▽), and 74 °C (■); (b) crystallized from the isotropic melt at $T_c = 72$ (○), 73 (▽), 74 (□), 75 (▽), 76 °C (●).

represent experimental data. In both cases a linear relation is obtained from the initial portion of the transformation in a double-logarithmic plot of the degree of transformation or as a function of the "degree of crystallinity" versus time. An integral value for n is found in both cases. The crystallizations of PBMOPP and PBMTTP show an (Avrami) exponent $n = 3$ (Figure 7a,b) in the free-growth approximation. Only at long crystallization times do deviations from the theory occur. The integral value $n = 3$ is related³⁸ to homogeneous nucleation and two-dimensional growth. Values of $n = 2.2, 2.4$ have been reported in other polyphosphazenes. In the analysis of PBEPP, a value of $n = 4$ has been found in this work (Figure 12). These differences in the (Avrami) exponent require further analysis. The conversion of the mesophase into the crystalline phase has been studied for some polyphosphazenes by Magill and co-workers^{13,22,29,30,39} using different experimental methods. These studies include dilatometry, calorimetry, SAXS, WAXS with a synchrotron high-intensity radiation source, and depolarized light intensity (DLI). These studies indicated an Avrami exponent $n = 2$ for the isotropic-mesogenic transformation and for the mesophase-crystalline transformation.³⁵

Another point of interest, related to the isotherm shape, was the level of crystallinity achieved at long times. It is important to realize that these polymers actually have an appreciable amorphous content, because in the thermal cycling, at temperatures below $T(1)$, they exhibit a glass transition temperature.

For this reason, the total crystallinity of PBMOPP was 65% (Figure 7a), and for PBMTTP it was 70% (Figure 7b). For PBEPP it was 35% (Figure 12a) when crystallizing from the mesophase and 70% when crystallizing from the isotropic melt (Figure 12b). These crystallinity levels were lower than those obtained by DSC from the cooling cycles from $T > T(1)$ to room temperature, except for PBMTTP. In the case of PBMOPP, the crystallinity was significantly lower than that obtained in the cooling cycle (82–90%). This last process and the subsequent heating cycle show a shoulder at 125 °C, which can be explained as a consequence of the wide molecular weight distribution. As has been shown, many polyphosphazenes have a very high molecular weight average and a broad distribution, even bimodal in some cases. The increase in crystallinity after isothermal transformation may be related to this situation. In the case of PBEPP crystallized from the mesophase, the crystallinity obtained from the DSC data is in the range 65–68%, higher than the value obtained from Figure 12a. The reasons for this difference are discussed above in the case of PBMOPP.

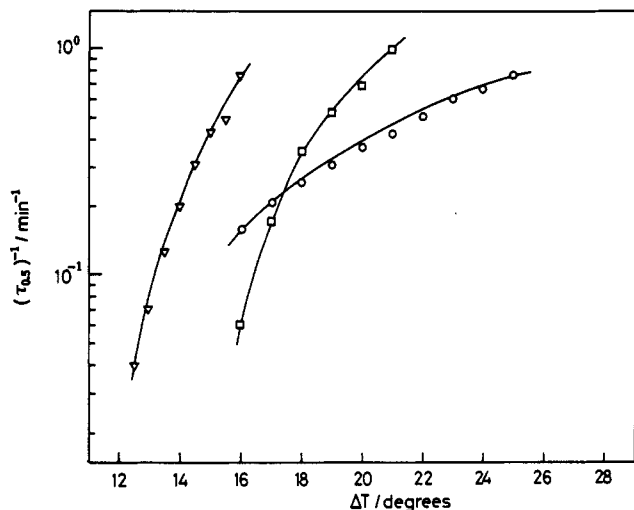


Figure 13. Plot of $\log(\tau_{0.5})^{-1}$ vs ΔT for PBMOPP (\square), PBMTTP (∇), and PBEPP (\circ).

As previously mentioned, the rate of the transformation was very dependent on the crystallization temperature and, therefore, on the undercooling, defined as $\Delta T = T(1) - T_c$. The transformation occurs at relatively low undercoolings. The half time $\tau_{0.5}$ (time to reach 50% of the conversion) obtained from the isotherms was plotted vs ΔT for the three polyphosphazenes (Figure 13). Like the crystallization of polymers from the amorphous state, the crystallization proceeds via the formation of crystalline nuclei and their subsequent growth. That is, the rate is very sensitive to the temperature and there is strong indication of a nucleation and growth mechanism in the transformation.

Magill³⁵ has pointed out that the larger the side groups, the less facile the overall crystallization process. At equivalent undercoolings, PBMTTP crystallized faster than PBMOPP, and PBEPP slower. In our case, differences in crystallization rates indicated that polarity played a more important role than the size of the attached group.

Additionally, the crystallization temperature coefficient can be analyzed, assuming a nucleation-controlled process. Although the transformation from the mesophase is not the same situation as isothermal crystallization from the melt (isotropic state), one can use the same formula in order to compare the experimental results. Thus, the rate at which crystallinity develops in terms of $\tau_{0.5}$ can be expressed by the general equation

$$\ln(\tau_{0.5})^{-1} = \ln(\tau_{0.5})_0^{-1} - K_2 T(1)/T\Delta T \quad (4)$$

for a two-dimensional nucleation mechanism.³⁹ In this equation

$$K_2 = 4\sigma_e\sigma_u/R\Delta H_u(T(1)) \quad (5)$$

where σ_e and σ_u are the interfacial free energy per repeat unit as it emerges from the basal plane of the nuclei and the lateral interfacial free energy, respectively.

According to eq 4, a plot of $\log(\tau_{0.5})^{-1}$ against $T(1)/T\Delta T$ should give a straight line with slope equal to K_2 . Figure 14 shows these plots for the three analyzed polyphosphazenes. Straight lines are obtained with the same slope for PBMOPP and PBMTTP, but with a significantly lower slope for PBEPP. The values obtained for $\sigma_e\sigma_u$ were 146.7 (cal/mol)² for PBMOPP, 85.2 (cal/mol)² for PBMTTP, and 19.7 (cal/mol)² for PBEPP. These values were lower than those obtained for poly[bis(trifluoroethoxy)phos-

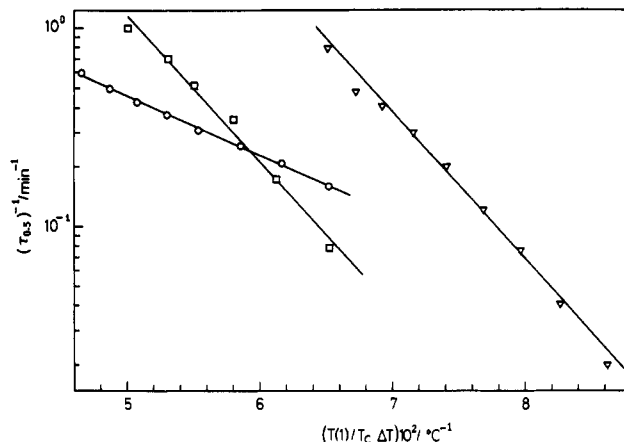


Figure 14. Plot of $\log(\tau_{0.5})^{-1}$ vs $T(1)/T\Delta T$ for PBMOPP (\square), PBMTTP (∇), and PBEPP (\circ).

phazene].²⁹ Nevertheless, they are comparable with the corresponding values of this product observed in polymer crystallization. Even the value for PBEPP was reasonable if the low heat of the transition for this polymer was considered.

In all the previous analysis, it has been held that $T(1)$ for each polyphosphazene was constant. However, Magill and co-workers²³ have indicated that $T(1)$ depends on the previous thermal history of the sample. The analysis of the transition temperature $T(1)$ after isothermal crystallization showed that, in these three polyphosphazenes, $T(1)$ does not change significantly in the relatively narrow range of crystallization temperatures that we have used. Differences in $T(1)$ were smaller than 1 °C and, therefore, a constant value of $T(1)$ has been used to calculate the operative undercooling.

Moreover, as previously mentioned, the temperature between $T(1)$ and T_m , from which the isothermal crystallization data are obtained, corresponded to a constant value for each polyphosphazene. Initially,¹³ different conditioning temperatures were assumed not to have a significant influence on the kinetics of the transformation. However, more recently²² it has been reported that changes in the previous conditioning temperature cause variations in the rate of the transformation. An increase in $\tau_{0.5}$ occurred when the temperature was raised. This dependence of the rate upon temperature in the $T(1)$ to T_m interval must be related to changes in polymer mobility.

In regard to this point, PBMOPP was crystallized at $T_c < T(1)$ from different T_r (preconditioning temperatures) above $T(1)$. For the same crystallization temperature, $\tau_{0.5}$ was smaller the higher was the preconditioning temperature. This fact represents a strong dependence of the crystallization kinetics on the conditions of the mesophase formation, in particular, the temperature at which the mesophase was held before crystallization. The increase in rate of crystallization seems to indicate that the structure of the mesophase became more ordered with heating, but this point deserves further study.

It is of considerable interest to compare the crystallization from the isotropic state with crystallization from the mesophase. The major limitation is that T_m and T_d (degradation) were too close for many polyphosphazenes, as is the case for PBMOPP and PBMTTP. However, PBEPP was a very favorable candidate for this type of study because $T_d \gg T_m$.

The isotherms obtained at $T_c < T(1)$ are plotted in Figure 12 for several crystallization temperatures. If $\tau_{0.5}$ values

were compared for the same crystallization temperature when the sample was crystallized from the mesomorphic state and from the isotropic state, it was found that crystallization was faster from the isotropic state. Moreover, the final crystallinity corresponded to 70% in this latter case. This value is much higher than the 35% that was found for crystallization from the mesomorphic state.

In order to discuss these results, it is important to mention a previous study of morphological changes in PBEPP.⁴⁰ When this polyphosphazene is quenched from the isotropic melt, there is no formation of the mesophase and only the crystallization at temperatures below $T(1)$ is observed. This indicates that the rate of mesophase formation is very low for this particular case. The morphology found for the crystalline polymer corresponds to spherulitic structures without any significant liquid crystalline order. That is, if the mesophase cannot be formed upon fast cooling from the isotropic melt, then the crystallization process was similar to that seen in other semicrystalline polymers.

However, when the crystallization occurred from the mesomorphic state, the anisotropic organization of the mesophase played an important role in the morphology. Crystalline lamellae with a random distribution in the anisotropic matrix were observed. The different morphologies were reflected not only in the crystallization rates that have been observed but also in the level of crystallinity that was attained.

Summary

We have analyzed the phase transitions observed in two new polyphosphazenes, and the results have been compared with new studies on PBEPP and other polyphosphazenes reported in the literature. The influence of the size and polarity of the substituents on the thermal transitions, interplanar spacings, and mesophase formation have been discussed. The kinetics of crystallization from the mesophase have also been analyzed. It has been shown that the rate of transformation depends very strongly on the sub- $(T(1))$ temperature. This fact has been interpreted as a nucleation and growth controlled process. The crystallization isotherms had similar behavior to that found in the crystallization of homopolymers, with an Avrami exponent $n = 3$ for PBMOPP and PBMTTP and $n = 4$ for PBEPP. With the assumption that the growth from the mesophase was similar to polymer crystallization, the temperature coefficient of the transformation process was determined. Values of this coefficient were related to the bulkiness and polarity of the substituents in these polyphosphazenes. Finally, the kinetics of the crystallization from the isotropic melt was also analyzed for the case of PBEPP.

Acknowledgment. We thank A. E. Tonelli for a critical reading of the manuscript. We gratefully acknowledge support for the work in Madrid by CICYT (MAT-88-0172).

References and Notes

- (1) Allcock, H. R.; Kugel, R. L.; Valan, K. J. *Inorg. Chem.* **1966**, *5*, 1709.
- (2) Allcock, H. R. *Phosphorus-Nitrogen Compounds*; Academic Press: New York, 1972.
- (3) Allcock, H. R. *Chem. Eng. News* **1985**, *63*, 22.
- (4) ACS Symp. Ser. **1988**, 360.
- (5) Schneider, N. S.; Desper, C. R.; Beres, J. J. In *Liquid Crystalline Order in Polymers*; Blumstein, A., Ed.; Academic Press: New York, 1978, Chapter 9.
- (6) Cheng, T. C.; Mochel, V. D.; Adams, H. E.; Longo, T. F. *Macromolecules* **1980**, *13*, 158.
- (7) Singler, R. E.; Schneider, N. S.; Hagnauer, G. L. *Polym. Eng. Sci.* **1975**, *15*, 34.
- (8) Schneider, N. S.; Desper, C. R.; Singler, R. E. *J. Appl. Polym. Sci.* **1976**, *12*, 566.
- (9) Alexander, M. N.; Desper, C. R.; Sagalyn, P. L.; Schneider, N. S. *Macromolecules* **1977**, *10*, 72.
- (10) Hagnauer, G. L.; Laliberte, B. R. *J. Appl. Polym. Sci.* **1976**, *20*, 3037.
- (11) Kojima, M.; Magill, J. H. *Polym. Commun.* **1983**, *24*, 329.
- (12) Kojima, M.; Magill, J. H. *Makromol. Chem.* **1985**, *186*, 649.
- (13) Magill, J. H.; Riekel, C. *Makromol. Chem., Rapid Commun.* **1986**, *7*, 287.
- (14) Allcock, H. R.; Arcus, R. A.; Stroh, E. G. *Macromolecules* **1980**, *13*, 919.
- (15) Kojima, M.; Masuko, T.; Magill, J. H. *Makromol. Chem., Rapid Commun.* **1988**, *9*, 565.
- (16) Kojima, M.; Magill, J. H. *Polym. Commun.* **1988**, *29*, 166.
- (17) Allcock, H. R.; Connolly, M. S.; Sisko, J. I.; Al-Shali, S. *Macromolecules* **1988**, *21*, 323.
- (18) Kojima, M.; Sun, D. C.; Magill, J. H. *Makromol. Chem.* **1989**, *190*, 1047.
- (19) Kojima, M.; Magill, J. H. *Polymer* **1989**, *30*, 1856.
- (20) Kojima, M.; Magill, J. H. *Polymer* **1989**, *30*, 579.
- (21) Godovsky, Y. K.; Papkov, V. S. *Adv. Polym. Sci.* **1989**, *88*.
- (22) Masuko, T.; Okuizumi, R.; Yonetake, K.; Magill, J. H. *Macromolecules* **1989**, *22*, 4636.
- (23) Sun, D. C.; Magill, J. H. *Polymer* **1987**, *28*, 1245.
- (24) Kojima, M.; Satake, H.; Masuko, T.; Magill, J. H. *J. Mater. Sci. Lett.* **1987**, *6*, 775.
- (25) Meille, S. V.; Porzio, W.; Allegra, G.; Audisio, G.; Gleria, M. *Makromol. Chem., Rapid Commun.* **1986**, *7*, 217.
- (26) Meille, S. V.; Porzio, W.; Bolognesi, A.; Gleria, M. *Makromol. Chem., Rapid Commun.* **1987**, *8*, 43.
- (27) Tanaka, H.; Gómez, M. A.; Tonelli, A. E.; Chichester-Hicks, S. V.; Haddon, R. C. *Macromolecules* **1988**, *21*, 2301.
- (28) Tanaka, H.; Gómez, M. A.; Tonelli, A. E.; Chichester-Hicks, S. V.; Haddon, R. C. *Macromolecules* **1989**, *22*, 1031.
- (29) Masuko, T.; Simeone, R. L.; Magill, J. H.; Plazek, D. J. *Macromolecules* **1984**, *17*, 2857.
- (30) Kojima, M.; Magill, J. H. *Polymer* **1985**, *26*, 1971.
- (31) Haddon, R. C.; Chichester-Hicks, S. V. *Macromolecules* **1989**, *22*, 1027.
- (32) Bowmer, T. N.; Haddon, R. C.; Chichester-Hicks, S. V.; Gómez, M. A.; Marco, C.; Fatou, J. G., in preparation.
- (33) Young, S. C.; Magill, J. H. *Macromolecules* **1989**, *22*, 2551.
- (34) Ergoz, E.; Fatou, J. G.; Mandelkern, L. *Macromolecules* **1972**, *5*, 147.
- (35) Magill, J. H. *Polym. Prepr. (Am. Chem. Soc., Div. Polym. Chem.)* **1989**, *30*, 297.
- (36) Avrami, M. *J. Chem. Phys.* **1939**, *7*, 1103.
- (37) Göler, V.; Sachs, F.; Sachs, G. *Z. Phys.* **1932**, *77*, 281.
- (38) Mandelkern, L. *Crystallization of Polymers*; McGraw-Hill: New York, 1964.
- (39) After submission of this paper, two new papers on the crystallization kinetics of polyphosphazenes appeared: (a) Ciora, R. J.; Magill, J. H. *Macromolecules* **1990**, *23*, 2350. (b) Ciora, R. J.; Magill, J. H. *Macromolecules* **1990**, *23*, 2359.
- (40) Gómez, M. A.; Marco, C.; Fatou, J. G.; Chichester-Hicks, S. V.; Haddon, R. C. *Polym. Commun.* **1990**, *31*, 308.